Graceful Vehicle Collision Avoidance using a Second-Order Nonlinear Barrier Constraint

Yejin Moon¹, Gábor Orosz², and Hosam K. Fathy^{1,*}

Abstract—This paper examines the problem of preventing frontal collisions between road vehicles. The paper focuses on the concept of achieving graceful safety control in the context of vehicle collision avoidance, in the sense of ensuring safety when possible, and degrading gracefully otherwise. This is achieved through a novel nonlinear barrier constraint which provides a multi-layered safety guarantee: it ensures safe spacing when possible, and avoids collision even when the safe spacing constraint is breached. The proposed graceful control approach is illustrated using a first-order barrier constraint. Then a second-order version of the constraint is presented that enables tracking a desired jerk signal while assuring graceful safety.

I. INTRODUCTION

Traffic accidents are among the leading causes of death worldwide, killing nearly 1.35 million people annually [1]. Approximately 94% of traffic accidents are caused by human drivers due to factors like drowsiness, distraction, etc. [2] [3]. These facts have historically motivated significant research on automotive safety control algorithms. Collision avoidance is an important problem for overall road safety, often addressed in the literature using control barrier functions. The use of barrier functions ensures that when a vehicle's state is initialized within a safe set (often representing a speed-dependent safe inter-vehicle distance), it remains within this set. This raises the question of how a safety algorithm should react when the above safe set is breached, perhaps due to an unsafe lane merger by a lead vehicle. This is addressed here by introducing the novel concept of graceful safety control.

Control barrier functions (CBFs) are widely utilized to guarantee the safety of dynamical systems. CBF methods have been applied broadly, including applications to automotive [4], [5], [6], robotic [7], [8], [9], [10], battery [11], [12], and biomedical systems [13], [14], [15]. CBF methods have at least two appealing features. First, they provide rigorous safety guarantees through the concept of forward invariance of a safe set in state space: the system can be guaranteed to remain within this set as long as it is initialized within it. Second, the CBF approach provides significant freedom in control design by allowing a controller to switch seamlessly between safety and other objectives, such as trajectory tracking [16], [17] or energy optimal behavior [18].

At least two types of barriers exist in the literature: reciprocal and zeroing CBFs [19], [20], [21]. A reciprocal CBF

tends to infinity as it approaches the boundary of the safe set, and remains finite within the interior of the safe set. Hence, by preventing the function from approaching infinity, one can guarantee safety. A zeroing CBF, in contrast, defines the safe set as the superlevel set, meaning that positive, negative, and zero values of the barrier function denote safety, its absence, and the boundary between those two conditions, respectively. Safety is then pursued by constraining the time derivative of the barrier function to ensure forward invariance [21].

For systems with a relative degree of one, that is, when the derivative of the CBF contains the control input, the input can be manipulated directly to satisfy the above constraint. For systems with a higher relative degree, exponential CBFs [22], higher-order CBFs [23] and backstepping [24] CBFs can be utilized. Such approaches have been extensively applied to guarantee the safety of systems where safety depends on position, but actuation directly affects acceleration [25], [26], [27], [28]. Within the automotive field, it is common to define safety in terms of the satisfaction of a velocity-dependent inter-vehicle spacing constraint [6], [28]. When this constraint is used for formulating a barrier function, vehicle acceleration appears in the time derivative of the constraint, thereby enabling longitudinal safety control.

The literature on the application of CBF methods to automotive safety includes collision and obstacle avoidance during racing [29], [30] and traffic congestion [31]; adaptive/connected cruise control with and without input delay [20], [32], [33]; human-vehicle trust dynamics [34]; lane-keeping control [4], [35]; and collision avoidance using differentiable and/or higher-order CBFs [25], [36], [37]. Throughout the above literature, the main focus is on ensuring forward invariance, meaning that if a system is initially in the safe set, then it always remains in the set. Scenarios when a system accidentally breaches a given safe set are relatively less explored. Consider, for example, a scenario where a lead vehicle "cuts off" an ego vehicle by changing lanes too close to the ego vehicle, as illustrated in Fig. 1. Suppose this maneuver breaches the ego vehicle's safe inter-vehicle spacing constraint. Can the ego vehicle avoid collision and recover gracefully from such a safety breach? If so, how can the vehicle's safety algorithm ensure such graceful control?

To the best of our knowledge, the above fundamental question – while profoundly important – has received very little attention in the literature. Our main goal in this paper is to address this gap by adding five novel contributions:

 First, we present an illustrative scenario in Section II, where classical CBF-based collision avoidance fails to react gracefully to a safety constraint breach. More

¹Yejin Moon and Hosam Fathy are with the Department of Mechanical Engineering, University of Maryland, College Park, MD 20742, USA. ²Gábor Orosz is with the Department of Mechanical Engineering and with the Department of Civil and Environmental Engineering, University of Michigan, MI 48109, USA. (Emails: ymoon@umd.edu, orosz@umich.edu, hfathy@umd.edu) *Corresponding author.

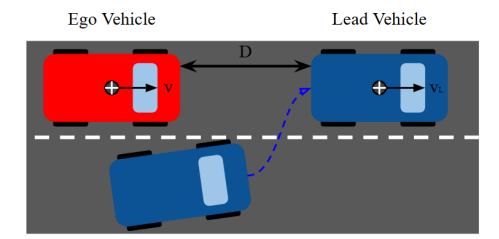


Fig. 1. Vehicle safety problem during a "cut off" maneuver.

specifically, we consider a scenario where a zeroing barrier function represents a minimum speed-dependent safe inter-vehicle distance. When the ego vehicle is "cut off" too aggressively, placing the initial condition outside the safe set, the CBF approach succeeds in gradually pushing the barrier function h back towards safety. However, this does not occur fast enough, and the inter-vehicle spacing drops to zero even as the value of the barrier function increases. The end result is that the traditional CBF approach, at least in this illustrative scenario, fails to prevent vehicle collision once the safe set is breached.

- Second, the paper introduces the novel notion of "graceful safety control". Specifically, in Section III we define a controller as graceful if it guarantees safety whenever possible, but avoids catastrophic safety incidents otherwise. The idea of graceful control has already been explored in the battery systems domain [12]. However, to the best of our knowledge, this paper represents the first application of this broad idea to automotive collision safety.
- Third, the paper develops a nonlinear barrier constraint that ensures graceful safety, as shown in Section III. The key idea is to create a multi-layered definition of safety. This differs from the classical delineation of safety in terms of the superlevel set of the zeroing barrier function, which creates a single definition of what it means to be in an unsafe state. In practice, safety is a multi-layered concept. For example, a true collision is clearly an extremely hazardous state that must be avoided. Excessive proximity to a lead vehicle, in contrast, is less hazardous and may be briefly tolerable provided the vehicles never collide and the spacing between them ultimately returns to the safe range. We define a safety controller as "graceful" if it is able to tolerate an unavoidable but slight worsening in safety, provided it avoids more extreme hazard states and is able to return to a truly safe state eventually.
- Fourth, we extend the above multi-layered definition of graceful safety to a second-order setting in Section IV.
 This makes it possible to construct a safety controller that assures convergence to safe inter-vehicle spacing while simultaneously attempting to track a smooth jerk trajectory.
- Finally, we demonstrate the above safety control strategy in simulation in Section V and summarize the conclusions in Section VI.

II. MOTIVATING EXAMPLE

Consider two vehicles separated by an inter-vehicle distance D, as shown in Fig. 1. If the longitudinal speeds of the ego and lead vehicles are v and $v_{\rm L}$, respectively, then the dynamics of inter-vehicle distance are given by:

$$\dot{D} = v_{\rm L} - v. \tag{1}$$

Now suppose that the spacing between these two vehicles can be deemed safe if it satisfies the following classical speed-dependent constraint from the literature (e.g. [20], [25], [28]):

$$D \ge D_{\rm sf} + T_{\rm sf}v. \tag{2}$$

Here, $D_{\rm sf}$ is the minimum inter-vehicle distance at zero speed and $T_{\rm sf}$ is a user-defined time headway. This safety constraint is designed to provide greater inter-vehicle spacing at higher speeds. It also ensures that vehicle acceleration appears in the resulting barrier constraint, as shown below. Given the above definition of vehicle safety, we construct the barrier function

$$h = D - D_{\rm sf} - T_{\rm sf}v,\tag{3}$$

whose positivity ensures safety.

Next, we pursue safety by imposing the following constraint at every instant in time [21]:

$$\dot{h} \ge -\alpha h.$$
 (4)

Substituting (1) and (3) into (4) gives

$$T_{\rm sf}\dot{v} \le v_{\rm L} - v + \alpha(D - D_{\rm sf} - T_{\rm sf}v). \tag{5}$$

We implement this safety constraint within a quadratic program, where the goal is to minimize vehicle acceleration \dot{v} (i.e., the control input) while ensuring safety:

$$\min_{\dot{v}} \frac{1}{2} \dot{v}^{2}
\text{s.t.} \quad T_{\text{sf}} \dot{v} \leq v_{\text{L}} - v + \alpha (D - D_{\text{sf}} - T_{\text{sf}} v).$$
(6)

Solving the above optimization problem at every instant in time provides a classical CBF-based vehicle safety guarantee. We simulate the behavior of the resulting illustrative benchmark safety controller below.

Consider a scenario where the ego vehicle implementing the above safety controller is initially traveling on a highway with speed $v(0)=30\,\mathrm{m/s}$. Suppose that a lead vehicle traveling at a much slower constant speed of $v_\mathrm{L}=10\,\mathrm{m/s}$ cuts the ego vehicle off. Moreover, suppose that the parameters of the above safety controller are given by $D_\mathrm{sf}=2\,\mathrm{m}$, $T_\mathrm{sf}=2\,\mathrm{s}$, and $\alpha=0.5\,\mathrm{s^{-1}}$. With these parameter values, safe inter-vehicle distance is set to 2 meters when the ego vehicle is stationary, and 62 meters at the above highway speed.

Fig. 2 plots the inter-vehicle spacing versus time for three different values of initial inter-vehicle distance D(0), namely, 10, 30, and 70 meters. Simulation is performed for a 5-second time window using the MATLAB *ode45* function, with 1 ms time step. The simulation stops as soon as the inter-vehicle distance hits zero, which represents collision. This occurs in the case where initial inter-vehicle spacing is $D(0)=10\,\mathrm{m}$.

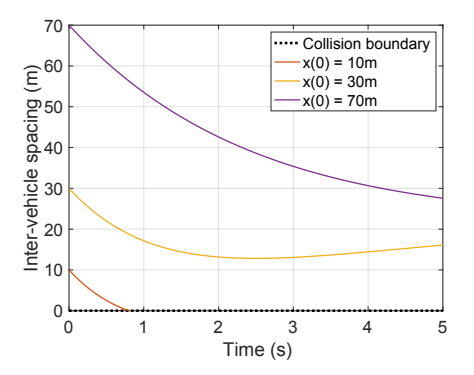


Fig. 2. Inter-vehicle distance for baseline controller

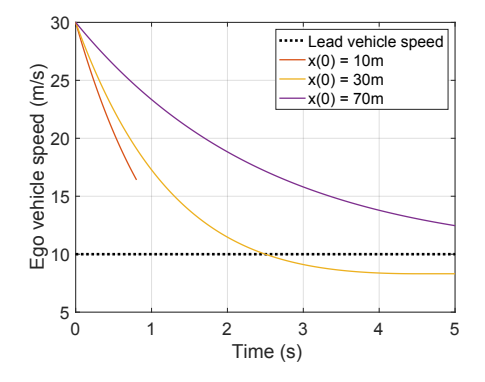


Fig. 3. Vehicle speed for baseline controller

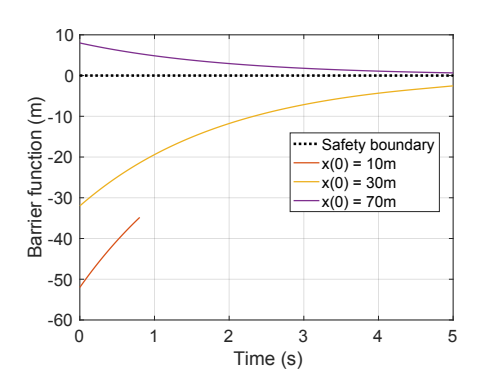


Fig. 4. Control barrier function for baseline controller

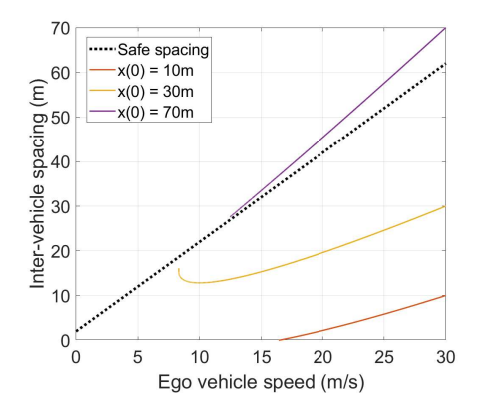


Fig. 5. Inter-vehicle distance vs. speed for baseline controller

The occurrence of the above collision is clearly an undesirable failure. This failure is not a result of physical limitations on parameters such as maximum vehicle braking capability. While such limitations do exist in practice, they are not accounted for in the above simple illustrative study. Moreover, this failure is not a consequence of the inability to achieve "safety" in the classical sense from the literature. As shown in Fig. 3, the ego vehicle does slow down for all three initial inter-vehicle distances. Furthermore, as shown in Fig. 4, the CBF does remain positive when it is initially positive, and does approach zero monotonically when it is initially negative. In other words, the safety controller performs as intended, yet the two vehicles collide anyway.

The true culprit behind the collision in this illustrative example is a fundamental limitation of the safety controller. This can be seen from Fig. 5, which presents a phase plane plot of inter-vehicle spacing versus ego vehicle speed. The dotted line represents the speed-dependent boundary in (2) between safe and unsafe inter-vehicle distances, hence the safe set is the domain above this line. When the initial intervehicle distance is above this line (i.e., when the system is initially safe), it remains above the line throughout the simulation. This is consistent with the goal of ensuring the forward invariance of the safe set. Moreover, when the initial inter-vehicle distance is below the dotted line, representing a safety violation, this violation diminishes with time, as desired.

Unfortunately, when the two vehicles are initially too close to each other, the safety controller does not reduce this safety violation fast enough to prevent collision. This is a fundamental failure arising from the lack of "grace" in the safety control problem formulation. A graceful controller should ideally prevent collision from occurring even when the safe inter-vehicle spacing constraint is breached. However, in this illustrative example, the controller fails to do so because it embraces a single-layer definition of safety, as opposed to a more graceful multi-layer definition.

III. GRACEFUL SAFETY CONTROL

This section presents the key idea behind the proposed graceful safety control approach. Specifically, this approach builds on the idea of defining safety as a multi-layer concept. This makes it possible to simultaneously tolerate and eventually alleviate hazardous inter-vehicle spacing, while applying progressively larger control inputs to avoid collision. This multi-layered approach brings together the core ideas behind both zeroing and reciprocal CBFs.

We begin by constructing a graceful control barrier function

$$h_{\rm g} = \frac{D}{s} \ge 1, \quad s = D_{\rm sf} + T_{\rm sf} v,$$
 (7)

where s is a speed-dependent safe inter-vehicle distance identical to the one used in the baseline controller, cf. (2). This barrier function definition is attractive because it provides two safety thresholds with distinct and important implications. A threshold exists at $h_{\rm g}=1$, below which inter-vehicle spacing is deemed unsafe and the recovery of safe spacing is

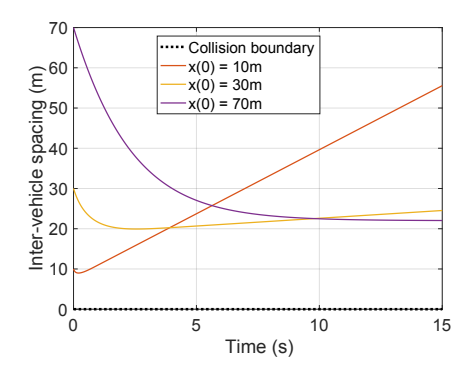


Fig. 6. Inter-vehicle distance for graceful controller

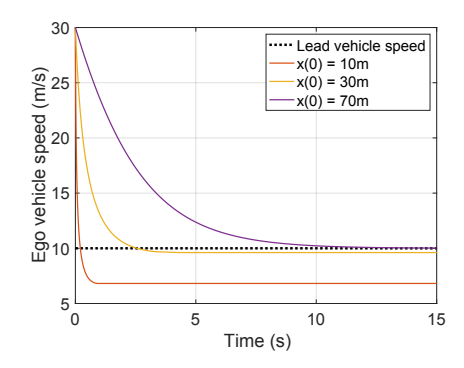


Fig. 7. Vehicle speed for graceful controller

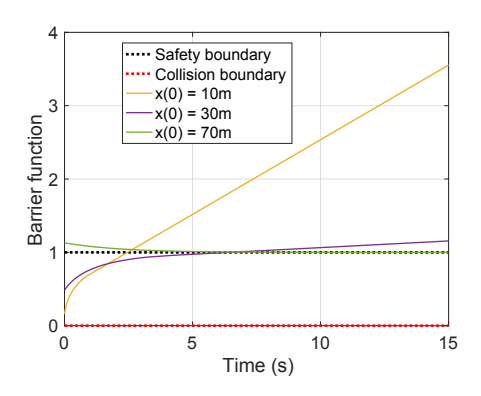


Fig. 8. Control barrier function for graceful controller

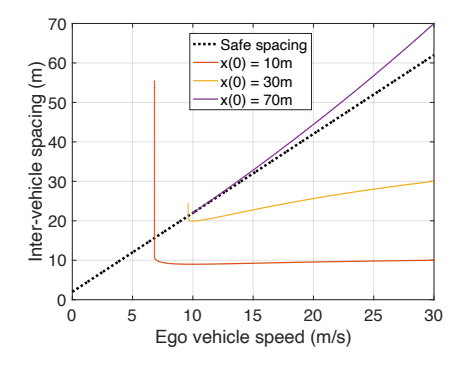


Fig. 9. Inter-vehicle distance vs. speed for graceful controller

desirable. A much more critical threshold exists at $h_{\rm g}=0$, below which collision occurs. Avoiding this latter threshold

is, therefore, truly essential for collision safety.

Imposing a constraint on the above barrier function can ensure graceful safety and guarantee the avoidance of the critical threshold at $h_{\rm g}=0$. For example, we propose the following novel first-order barrier constraint

$$\dot{h}_{\rm g} \ge \alpha \left(\frac{1}{h_{\rm g}} - 1\right),$$
 (8)

which provides a "stiffening effect" tailored to ensure the avoidance of $h_{\rm g}=0$. A rigorous proof of this graceful safety guarantee is intended for presentation in a subsequent publication, but the core idea behind this proof is that the proposed graceful control law acts as a zeroing CBF around $h_{\rm g}=1$ and as a reciprocal CBF around $h_{\rm g}=0$.

Substituting (7) into (8) gives

$$\dot{v} \le \frac{1}{DT_{\rm sf}} \left(s(v_{\rm L} - v) + \alpha s^2 \left(1 - \frac{s}{D} \right) \right), \quad s = D_{\rm sf} + T_{\rm sf} v.$$
(9)

We implement this constraint within a quadratic program, where the goal is to minimize vehicle acceleration \dot{v} (i.e., the control input) while ensuring graceful safety:

$$\min_{\dot{v}} \frac{1}{2} \dot{v}^{2}$$
s.t. $\dot{v} \leq \frac{1}{DT_{\text{sf}}} \left(s(v_{\text{L}} - v) + \alpha s^{2} \left(1 - \frac{s}{D} \right) \right),$

$$s = D_{\text{sf}} + T_{\text{sf}} v.$$
(10)

Implementing the above quadratic program at every time instant leads to graceful safety control, as shown in the simulation example below.

The same simulation setup as for the benchmark controller case is used. Again, the simulation was performed using the MATLAB *ode45* function, with a 1 ms time step, but a longer time horizon of 15 seconds is used here.

Figure 6 plots the inter-vehicle spacing versus time when the above graceful controller is used, for the same parameter values used in the baseline simulation study. The benefits of graceful control are immediately clear: regardless of initial inter-vehicle spacing, collision never occurs. The ego vehicle always slows down sufficiently fast to avoid such a catastrophe, as shown in Fig. 7.

The above behavior is a direct consequence of graceful control design. As shown in Fig. 8, the graceful controller tolerates hazardous inter-vehicle distances, but reduces them over time by bringing the value of $h_{
m g}$ closer to the safety threshold value of 1. In addition, under no circumstances does the controller allow the value of $h_{
m g}$ to reach the catastrophic value of 0. This behavior can also be seen in the phase plane plot in Fig. 9, where undesirable deviations from safe inter-vehicle spacing are reduced very quickly. The speed with which this is done prevents collisions. In fact, the vehicle brakes harder and decelerates more aggressively for smaller initial values of inter-vehicle spacing, thereby always avoiding collisions. Interestingly, once collisions are avoided, the ego vehicle returns to zero acceleration, and the phase plane plots become vertical. From this event onward, intervehicle spacing becomes safer as the lead vehicle pulls away.

IV. GRACEFUL CONTROL DESIGN

The above simulation example highlights the power and importance of graceful control. By intentionally introducing a two-layer definition of safety, graceful control combines the power of zeroing and reciprocating CBFs. Like zeroing CBFs, graceful control slowly returns to safety when the safe inter-vehicle spacing constraint is breached. Moreover, like reciprocating CBFs, graceful control ensures that intervehicle collisions never occur. That said, the simulation example has at least three limitations from a practical perspective. First, no constraints are imposed on vehicle deceleration in this illustrative example, for simplicity. Second, the optimization objective in the example is to minimize acceleration, as opposed to tracking a desired cruise control trajectory. Finally, no effort is made in the above simple example to minimize jerk or track a smooth desired jerk trajectory. This is undesirable given the degree to which vehicle jerk affects passenger comfort.

The main goal of this section is to extend the idea of graceful vehicle safety control in a manner that addresses the above limitations. This furnishes a more practical graceful controller, one that utilizes a second-order barrier constraint instead of a first-order constraint.

We begin by creating a baseline cruise controller that prevents excessive jerk while tracking the lower of the two velocity values: a desired velocity $v_{\rm max}$ set by the user and the lead vehicle's velocity $v_{\rm L}$. That is, we define the speed policy [28]:

$$W(v_{\rm L}) = \min\{v_{\rm L}, v_{\rm max}\}. \tag{11}$$

This policy is not intended to ensure graceful safety control. Rather, the intent is to provide a reference jerk signal at every moment in time for the graceful controller to track if possible. We define the proposed cruise controller as the solution to the following second-order differential equation

$$\ddot{v}_{c} + 2\zeta_{c}\omega_{c}\dot{v} + \omega_{c}^{2}(v - W(v_{L})) = 0, \tag{12}$$

where $\ddot{v}_{\rm c}$ denotes a desired target value for the vehicle's jerk. The design parameters are the natural frequency $\omega_{\rm c}>0$ and the damping ratio $\zeta_{\rm c}>0$. At equilibrium, this oscillator converges to the desired vehicle speed $v_{\rm max}$ or $v_{\rm L}$, cf. (11).

We assume that there is a known lower bound a_{\min} on vehicle acceleration corresponding to the maximum braking ability of the ego vehicle. This results in the inequality constraint

$$\dot{v} \ge a_{\min}.$$
 (13)

We honor this constraint in a manner that is analogous to zeroing CBF theory. Namely, we rewrite the constraint as

$$H(\dot{v}) = \dot{v} - a_{\min} \ge 0,\tag{14}$$

and impose the CBF-like constraint

$$\dot{H} \ge -\gamma H \implies \ddot{v} \ge -\gamma (\dot{v} - a_{\min}),$$
 (15)

on the time derivative of the function H. The intent is to guarantee that if the vehicle deceleration is initially feasible, it will remain feasible at all subsequent moments in time.

The minimum acceleration a_{\min} can be computed from the vehicle's longitudinal dynamics as

$$a_{\min} = -\frac{1}{m} \left(F_{\text{br}} + \frac{1}{2} C_{\text{d}} \rho A_{\text{f}} v^2 + C_{\text{r}} m g \right),$$
 (16)

where m is the mass of the vehicle, $F_{\rm br}>0$ is the largest braking force applicable, $C_{\rm d}$ is the air drag coefficient, ρ is the air density, $A_{\rm f}$ is the vehicle's frontal area, $C_{\rm r}$ is the rolling resistance coefficient, and g is the acceleration of gravity. The values of these parameters are given in Table I.

The final step towards the proposed controller is to extend the graceful control barrier constraint from first to second order. One way to achieve this is to construct a graceful safety constraint of the form

$$\ddot{h}_{\rm g} + 2\zeta_{\rm s}\omega_{\rm s}\dot{h}_{\rm g} + \omega_{\rm s}^2 \left(1 - \frac{1}{h_{\rm g}}\right) \ge 0,\tag{17}$$

where the graceful barrier function $h_{\rm g}$ is given in (7), while the natural frequency $\omega_{\rm s}>0$ and the damping ratio $\zeta_{\rm s}>0$ are design parameters. The damping ratio $\zeta_{\rm s}$ does not have to be greater than or equal to one: a fact that provides greater freedom in designing the safety controller. The nonlinearity in $\omega_{\rm s}^2(1-1/h_{\rm g})$ provides a stiffening effect that ensures the avoidance of $h_{\rm g}=0$, see the analogous stiffening term in the first-order safety constraint (8). In fact, the spirit of both constraints is to design a safety controller that is analogous to a zeroing CBF around $h_{\rm g}=1$, and analogous to a reciprocal CBF around $h_{\rm g}=0$. This provides the multi-layered safety mindset that is central to graceful safety control.

The proposed second-order graceful controller assembles the above equations into the quadratic program

$$\min_{\ddot{v},\epsilon} \frac{1}{2} (\ddot{v} - \ddot{v}_{c})^{2} + \frac{1}{2} w_{p} \epsilon^{2}$$
s.t.
$$\ddot{v}_{c} + 2\zeta_{c} \omega_{c} \dot{v} + \omega_{c}^{2} (v - W(v_{L})) = 0,$$

$$\ddot{v} \geq -\gamma (\dot{v} - a_{\min}),$$

$$\ddot{h}_{g} + 2\zeta_{s} \omega_{s} \dot{h}_{g} + \omega_{s}^{2} \left(1 - \frac{1}{h_{g}}\right) + \epsilon \geq 0,$$

$$h_{g} = \frac{D}{D_{sf} + T_{sf} v},$$

$$\epsilon \geq 0.$$
(18)

Here, the main optimization goal is to minimize the deviation between the actual vehicle jerk and the jerk needed to track the cruise control law. This optimization is performed subject to the reference cruise control dynamics, the acceleration limit, and the condition on the graceful control barrier function. The latter two are inequality constraints which both impose bounds on jerk and these may be mutually conflicting. This is addressed by introducing the positive slack variable ϵ in the barrier condition, and adding ϵ^2 to the optimization objective with some Pareto weight $w_{\rm p}$.

Solving the above quadratic program at every instant in time furnishes a second-order version of the proposed graceful safety controller. This controller retains the ability to achieve graceful safety, with the added benefit of addressing the practical challenges listed at the beginning of this section.

TABLE I LIST OF PARAMETER VALUES

Symbol	Definition	Value
$\zeta_{ m s}$	Graceful controller damping ratio	0.1
$\omega_{ m s}$	Graceful controller frequency	2 rad/s
$\zeta_{ m c}$	Jerk equation damping ratio	1.1
$\omega_{ m c}$	Jerk equation natural frequency	1 rad/s
γ	Jerk barrier function time constant	$5 {\rm s}^{-1}$
$T_{\rm sf}$	Safe time headway	1.5 s
$D_{\rm sf}$	Minimum inter-vehicle distance	2 m
$F_{ m br}$	Maximum braking force	8436.6 N
ρ	Air density	1.22 kg/m^3
A_{f}	Car frontal area	2 m^2
$C_{\rm d}$	Drag coefficient	0.35
$C_{\rm r}$	Rolling resistance coefficient	0.01
g	Gravitational acceleration	9.81 m/s^2
$w_{ m p}$	Pareto weight	100

V. SIMULATION RESULTS

In this section, we evaluate the proposed graceful safety controller for two different cut-in scenarios over a 30-second time horizon. In both scenarios, the ego vehicle drives at the initial velocity of $v(0)=26.8~\mathrm{m/s}$. At t=0, the lead vehicle cuts in front of the ego vehicle at a speed of $v_{\rm L}(0)=17~\mathrm{m/s}$, with an inter-vehicle distance of $D(0)=15~\mathrm{meters}$. The initial acceleration of the ego vehicle is set to $\dot{v}(0)=0~\mathrm{m/s^2}$. The desired velocity set by the user is assumed to be $v_{\rm max}=24~\mathrm{m/s}$ while the other parameters are listed in Table I. The time step used is set to 0.01 seconds and Matlab's quadprog function is utilized for solving the quadratic program (18).

In the first scenario, after cutting into the lane of the ego car, the lead vehicle maintains its speed for 3 seconds. Then, this vehicle accelerates at the rate of 1 m/s² until it reaches 26.8 m/s. Fig. 10 plots the vehicles' velocity profiles, intervehicle distance, and barrier function. The desired velocity curve shows the target velocity $W(v_{\rm L})$ of the adaptive cruise controller, see (11). The safe distance in the middle panel is obtained by calculating $D_{\rm sf} + T_{\rm sf}v$, see (7). Fig. 11 depicts the ego vehicle's acceleration, jerk, and slack variable over time. In the middle panel the desired jerk $\ddot{v}_{\rm c}$ is also depicted.

The inter-vehicle distance starts below the safe distance. The graceful barrier function, as a result, starts at a value between 0 and 1 – the state that is still considered undesirable. Therefore, the controller decreases the ego car's acceleration and jerk to reduce the velocity. The vehicle's acceleration rapidly drops to its minimum bound. However, the vehicle jerk stays above the value of $-10~\rm m/s^3$. This reasonable jerk drives the graceful barrier function to a value close to zero. Yet, since the controller maintains the deceleration for about 4 seconds, the vehicle is able to sufficiently decrease its velocity, recover the safe inter-vehicle distance, and start tracking the desired velocity set by the user for the rest of the time horizon.

In the second scenario, after cutting in, the lead vehicle maintains its speed for the first 3 seconds, then slows down at a rate of $1~\mathrm{m/s^2}$ until it reaches $10~\mathrm{m/s}$. Fig. 12 plots the vehicles' velocity profiles, inter-vehicle distance, and barrier

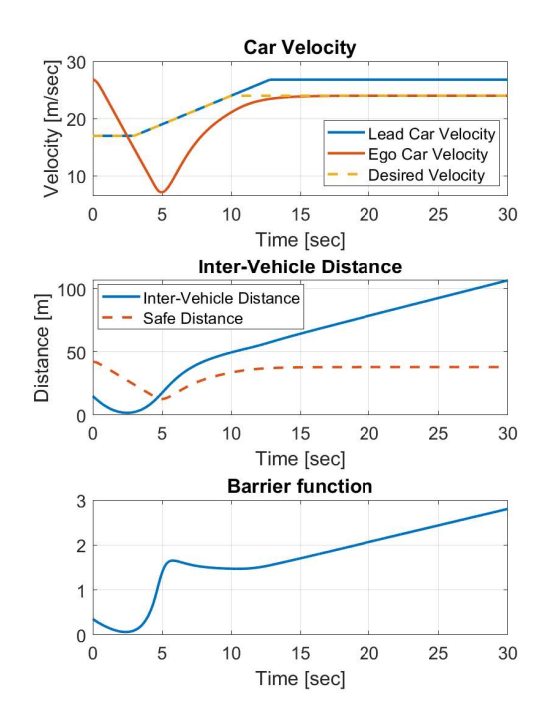


Fig. 10. Velocity, inter-vehicle distance, and barrier function for the scenario when the lead vehicle speeds up after the cut off

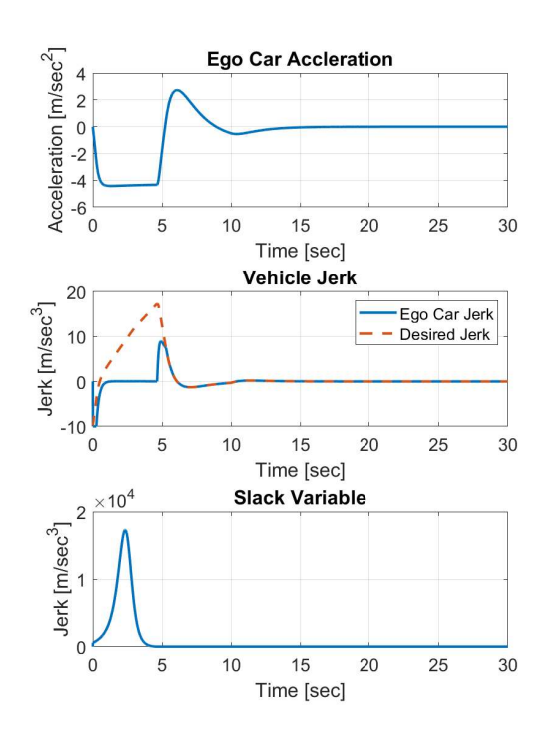


Fig. 11. Acceleration, jerk, and slack variable for the scenario when the lead vehicle speeds up after the cut off

function while Fig. 13 depicts the ego vehicle's acceleration, jerk, and slack variable over time. Similar to the previous scenario, the distance and the barrier function start at an

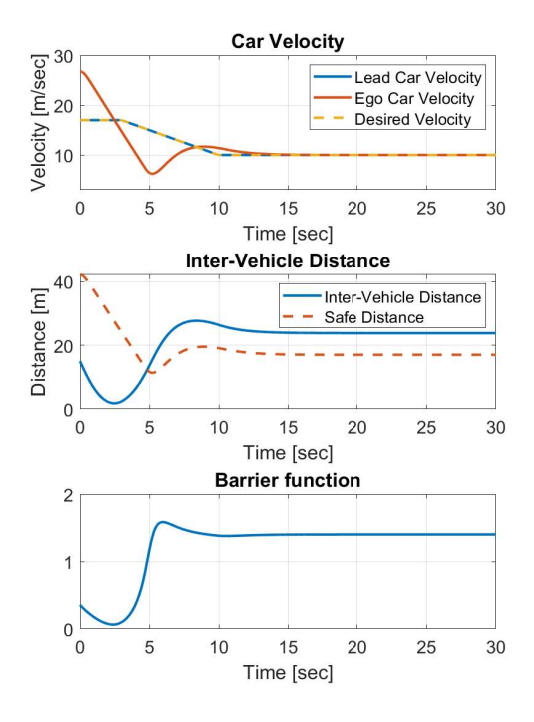


Fig. 12. Velocity, inter-vehicle distance, and barrier function for the scenario when the lead vehicle slows down after the cut off

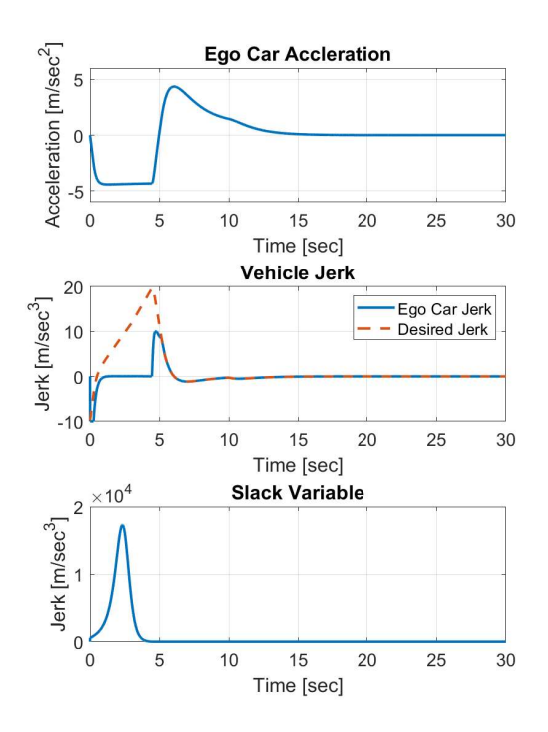


Fig. 13. Acceleration, jerk, and slack variable for the scenario when the lead vehicle slows down after the cut off

undesirable state and then become slightly worse for the first 3 seconds. However, as the car decelerates at its maximum rate, the system soon becomes safe and starts tracking the

lead car's velocity, while still maintaining a reasonable jerk value. These simulation results again highlight the benefits of the graceful safety controller, particularly its ability to avoid collision even when starting from unsafe inter-vehicle distances.

VI. CONCLUSION

Perhaps the most important conclusion from this paper is a fundamental insight into one of the core limitations of classical safety control theory, as well as one potential remedy for this limitation. In classical safety control, the underlying single-layer definition of safety lacks grace. When the single dividing line between safe and hazardous scenarios is breached, recovery from this breach may not be fast enough to ensure collision avoidance. This is a result of the speed-dependent definition of safe inter-vehicle spacing, together with the single-layer definition of the resulting safety barrier function. By providing a multi-layer approach to safety, graceful control prevents inter-vehicle collisions even when safe vehicle spacing constraints are breached.

ACKNOWLEDGMENT

Support for this research was provided by the U.S. National Science Foundation. The authors gratefully acknowledge this support. This paper reflects the opinions of the authors, not the U.S. National Science Foundation.

REFERENCES

- World Health Organization, Global Status Report on Road Safety, 2015.
- [2] A. Eskandarian, C. Wu, and C. Sun, "Research advances and challenges of autonomous and connected ground vehicles," *IEEE Transactions on Intelligent Transportation Systems*, vol. 22, no. 2, pp. 683–711, 2019.
- [3] J. Chen, H. Liang, J. Li, and Z. Lv, "Connected automated vehicle platoon control with input saturation and variable time headway strategy," *IEEE Transactions on Intelligent Transportation Systems*, vol. 22, no. 8, pp. 4929–4940, 2020.
- [4] X. Xu, J. W. Grizzle, P. Tabuada, and A. D. Ames, "Correctness guarantees for the composition of lane keeping and adaptive cruise control," *IEEE Transactions on Automation Science and Engineering*, vol. 15, no. 3, pp. 1216–1229, 2017.
- [5] H. Ma, J. Chen, S. E. Li, Z. Lin, Y. Guan, Y. Ren, and S. Zheng, "Model-based constrained reinforcement learning using generalized control barrier function," in *IEEE/RSJ International Conference on Intelligent Robots and Systems (IROS)*. IEEE, 2021, pp. 4552–4559.
- [6] A. Alan, A. J. Taylor, C. R. He, A. D. Ames, and G. Orosz, "Control barrier functions and input-to-state safety with application to automated vehicles," *IEEE Transactions on Control Systems Technology*, 2023
- [7] W. Xiao, T.-H. Wang, R. Hasani, M. Chahine, A. Amini, X. Li, and D. Rus, "Barriernet: Differentiable control barrier functions for learning of safe robot control," *IEEE Transactions on Robotics*, vol. 39, no. 3, pp. 2289–2307, 2023.
- [8] A. Agrawal and K. Sreenath, "Discrete control barrier functions for safety-critical control of discrete systems with application to bipedal robot navigation." in *Robotics: Science and Systems*, vol. 13, 2017, pp. 1–10.
- [9] Z. Gao, G. Yang, and A. Prorok, "Learning environment-aware control barrier functions for safe and feasible multi-robot navigation," arXiv preprint arXiv:2303.04313, 2023.
- [10] D. Panagou, D. M. Stipanovič, and P. G. Voulgaris, "Multi-objective control for multi-agent systems using lyapunov-like barrier functions," in 52nd IEEE Conference on Decision and Control. IEEE, 2013, pp. 1478–1483.

- [11] S. D. Vyas, T. Roy, and S. Dey, "Thermal fault-tolerance in lithium-ion battery cells: A barrier function based input-to-state safety framework," in *IEEE Conference on Control Technology and Applications (CCTA)*. IEEE, 2022, pp. 1178–1183.
- [12] Y. Moon and H. K. Fathy, "Graceful safety control: Motivation and application to battery thermal runaway," *IFAC-PapersOnLine*, vol. 58, no. 28, pp. 666–671, 2024.
- [13] A. D. Ames, T. G. Molnár, A. W. Singletary, and G. Orosz, "Safety-critical control of active interventions for COVID-19 mitigation," *IEEE Access*, vol. 8, pp. 188454–188474, 2020.
- [14] Y. Moon, B. KadkhodaeiElyaderani, J. Leibowitz, P. Rezaei, E. M. Abdelazim, M. Awad, S. Stachnik, S. Stewart, J. S. Friedberg, J.-O. Hahn et al., "Safe model-based multivariable control of peritoneal perfusion," *IFAC-PapersOnLine*, vol. 56, no. 3, pp. 301–306, 2023.
- [15] W. Yin, H. K. Fathy, and J.-O. Hahn, "Safe automation of interfering medical treatments via control barrier functions and reachability analysis: a fluid resuscitation-sedation-vasopressor infusion case study," *Journal of Clinical Monitoring and Computing*, pp. 1–18, 2025.
- [16] P. Wieland and F. Allgöwer, "Constructive safety using control barrier functions," *IFAC Proceedings Volumes*, vol. 40, no. 12, pp. 462–467, 2007.
- [17] B. G. Goswami, M. Tayal, K. Rajgopal, P. Jagtap, and S. Kolathaya, "Collision cone control barrier functions: Experimental validation on ugvs for kinematic obstacle avoidance," in *American Control Conference (ACC)*. IEEE, 2024, pp. 325–331.
- [18] A. Alan, C. R. He, T. G. Molnár, J. C. Mathew, A. H. Bell, and G. Orosz, "Integrating safety with performance in connected automated truck control: Experimental validation," *IEEE Transactions on Intelligent Vehicles*, vol. 9, no. 1, pp. 3075–3088, 2024.
- [19] A. D. Ames, S. Coogan, M. Egerstedt, G. Notomista, K. Sreenath, and P. Tabuada, "Control barrier functions: Theory and applications," in *European Control Conference (ECC)*. IEEE, 2019, pp. 3420–3431.
- [20] A. D. Ames, J. W. Grizzle, and P. Tabuada, "Control barrier function based quadratic programs with application to adaptive cruise control," in 53rd IEEE Conference on Decision and Control. IEEE, 2014, pp. 6271–6278
- [21] A. D. Ames, X. Xu, J. W. Grizzle, and P. Tabuada, "Control barrier function based quadratic programs for safety critical systems," *IEEE Transactions on Automatic Control*, vol. 62, no. 8, pp. 3861–3876, 2017.
- [22] Q. Nguyen and K. Sreenath, "Exponential control barrier functions for enforcing high relative-degree safety-critical constraints," in *American Control Conference (ACC)*. IEEE, 2016, pp. 322–328.
- [23] W. Xiao and C. Belta, "Control barrier functions for systems with high relative degree," in 58th IEEE Conference on Decision and Control (CDC). IEEE, 2019, pp. 474–479.
- [24] M. H. Cohen, T. G. Molnár, and A. D. Ames, "Safety-critical control for autonomous systems: Control barrier functions via reduced-order models," *Annual Reviews in Control*, vol. 57, p. 100947, 2024.
- [25] G. Gunter and D. Work, "Safe driving with control barrier functions in mixed autonomy traffic when cut-ins occur," in *European Control Conference (ECC)*. IEEE, 2022, pp. 411–416.
- [26] S. Van Koevering, Y. Lyu, W. Luo, and J. Dolan, "Provable probabilistic safety and feasibility-assured control for autonomous vehicles using exponential control barrier functions," in *IEEE Intelligent Vehicles Symposium (IV)*. IEEE, 2022, pp. 952–957.
- [27] A. Ghaffari and M. Desai, "Exponential barrier functions for safe steering of nonholonomic vehicles with actuator time-delay," *IEEE Access*, vol. 10, pp. 9184–9197, 2022.
- [28] T. G. Molnár, G. Orosz, and A. D. Ames, "On the safety of connected cruise control: analysis and synthesis with control barrier functions," in 62nd IEEE Conference on Decision and Control (CDC). IEEE, 2023, pp. 1106–1111.
- [29] G. Notomista, M. Wang, M. Schwager, and M. Egerstedt, "Enhancing game-theoretic autonomous car racing using control barrier functions," in *IEEE International Conference on Robotics and Automation (ICRA)*. IEEE, 2020, pp. 5393–5399.
- [30] J. Zeng, B. Zhang, and K. Sreenath, "Safety-critical model predictive control with discrete-time control barrier function," in *American Control Conference (ACC)*. IEEE, 2021, pp. 3882–3889.
- [31] R. Cheng, G. Orosz, R. M. Murray, and J. W. Burdick, "End-to-end safe reinforcement learning through barrier functions for safety-critical continuous control tasks," in 33rd AAAI Conference on Artificial Intelligence, 2019, pp. 3387–3395.

- [32] C. I. Chinelato and B. A. Angélico, "Safe adaptive cruise control with control barrier function and smith predictor," in *Congresso Brasileiro* de Automática, vol. 2, no. 1, 2020.
- [33] A. K. Kiss, T. G. Molnár, A. D. Ames, and G. Orosz, "Control barrier functionals: Safety-critical control for time delay systems," *International Journal of Robust and Nonlinear Control*, vol. 33, no. 12, pp. 7282–7309, 2023.
- [34] C. Hu and J. Wang, "Trust-based and individualizable adaptive cruise control using control barrier function approach with prescribed performance," *IEEE Transactions on Intelligent Transportation Systems*, vol. 23, no. 7, pp. 6974–6984, 2021.
- [35] C. Jiang, H. Gan, I. Vörös, D. Takács, and G. Orosz, "Safety filter for lane-keeping control," in *Advanced Vehicle Control Symposium*. Springer, 2024, pp. 371–377.
- [36] W. Xiao, T.-H. Wang, M. Chahine, A. Amini, R. Hasani, and D. Rus, "Differentiable control barrier functions for vision-based end-to-end autonomous driving," arXiv preprint arXiv:2203.02401, 2022.
- [37] Y. Chen, G. Orosz, and T. G. Molnár, "Safety-critical connected cruise control: leveraging connectivity for safe and efficient longitudinal control of automated vehicles," in 27th IEEE International Conference on Intelligent Transportation Systems. IEEE, 2024.